Bernal-Casas et al., J Child Adolesc Behav 2015, 3:5
DOI: 10.4172/2375-4494.1000248

Journal of Child & Adolescent Behavior

Research Article Open Access

Altered Structural-functional Maturation of the Right Amygdala in Healthy Adolescents Exposed to Traumatic Events

Bernal-Casas D[1]*, Pincham H[2], Harding E[2], Prabhu G[1], Fearon P[2,3] and Dolan R[1]

[1]*Department of Neurology, Wellcome Trust Centre for Neuroimaging, Institute of Neurology, University College London, London, UK*
[2]*Department of Neurology, Developmental Neuroscience Unit, The Anna Freud Centre, UK*
[3]*Department of Clinical Research, Educational and Health Psychology, University College London, UK*

Abstract

Trauma is defined as a physical or psychological threat or assault to an individual's physical integrity, sense of self, safety or survival or to the physical safety of a significant other. The most common long-term mental health conditions resulting from trauma are post-traumatic stress disorder (PTSD) and depression. A number of studies using neuroimaging methodologies have implicated the amygdala and hippocampus in emotion processing in mood disorders, and adult depression studies suggest amygdala-hippocampal functional connectivity deficits. However, while trauma contributes to depression in a variety of ways, the neurobiological mechanisms underlying exposure to traumatic experiences have been poorly studied. In order to address this question, we used voxel based morphometry (VBM) and spectral dynamic causal modelling (spectral DCM; spDCM) approaches to analyse structural and resting-state functional magnetic resonance imaging and examine grey matter volume, white matter volume, and effective connectivity within the amygdala-hippocampal network in adolescents without psychiatric diagnoses, who had or had not been previously exposed to traumatic life events. Our results indicated greater intrinsic connectivity within the right amygdala in individuals with traumatic experiences compared to controls. Likewise we observed reduced white matter volume within the same region in those individuals, compared with controls. Together, these findings are suggestive of altered maturation of the right amygdala in healthy adolescents following trauma exposure. We interpret such brain changes as a plausible mechanism that may make individuals more vulnerable to developing psychopathology later in life.

Keywords: MRI; Structural MRI; Resting-state fMRI (rs-fMRI); VBM; Spectral DCM; Amygdala; Hippocampus; Trauma

Introduction

Exposure to traumatic life events and experiences during childhood is associated with an increased risk of later psychopathology, as well as impaired neurobiological and neurocognitive functioning [1,2]. Even though the neurobiological mechanisms remain poorly understood, there is likely a complex interplay between environmental experiences and individual differences in risk versus protective genes, which influence the brain circuitry underpinning psychological and emotional development [3]. Stressful events in childhood and adolescence are proposed to alter outputs of the hypothalamic-pituitary-adrenal axis, resulting in sustained high levels of glucocorticoid steroids. The structure and function of the limbic system, specifically the hippocampus and amygdala, appear particularly vulnerable to these changes [4]. For instance, reduced hippocampal volumes in adults with PTSD and a history of childhood physical and sexual abuse has been reported [5]. Further, reduced resting-state functional connectivity between the right amygdala and a number of limbic structures, including the hippocampus and putamen, in individuals drawn from the Netherlands Study of Depression and anxiety was found [6]. Notably, much existing research has examined alterations in the neural architecture of patient cohorts, such as those with post-traumatic stress disorder [5,7-13] or trauma-induced depression [14]. Notwithstanding the usefulness of these studies, it is important to consider whether the same findings hold in young people who have been exposed to stressful life events but are currently free of comorbid psychopathology. This is important to enable the comparison between trauma-exposed and non-exposed participants to be matched for current psychopathology. To that end, the current study was interested in whether young people who have previously experienced a stressful life event (but are currently psychologically well) demonstrate abnormalities in either brain structure or functional connectivity compared to an age-matched control group.

A number of studies have examined structural brain changes following trauma exposure in individuals without psychiatric diagnoses. While many have reported volumetric reductions in the hippocampus [15-17] or amygdala [18], others have found no change in either hippocampal or amygdala volume [19,20]. Resting-state functional imaging studies have also produced varied results, with some research reporting increased amygdala-hippocampal connectivity associated with greater levels of self-reported trauma symptoms [21] or following stress induction [22], and other work reporting no trauma-related connectivity changes [18]. Variability in type of trauma exposure, and imaging analysis may play a role in explaining these discrepancies. Through the use of combined structural and functional measures, we aimed to contribute understanding on the relevance of amygdala-hippocampal interactions in trauma exposure.

Our focus on young people was driven by the notion that trauma exposure is likely to be most influential in shaping neural structures during developmentally sensitive periods [23,24]. Adolescence is a sensitive period for both cognitive and neural development [25], and is associated with an increased incidence of psychiatric disorder

***Corresponding author:** Bernal-Casas D, Department of Neurology, Wellcome Trust Centre for Neuroimaging, Institute of Neurology, University College London, 12 Queen Square - London - WC1N 3BG, UK, Tel: +44 (0) 20 3448 4362; Fax: +44 (0) 20 7813 1420; E-mail: bernalgps@gmail.com

Received August 11, 2015; **Accepted** September 15, 2015; **Published** September 22, 2015

Citation: Bernal-Casas et al. (2015) Altered Structural-functional Maturation of the Right Amygdala in Healthy Adolescents Exposed to Traumatic Events. J Child Adolesc Behav 3: 248. doi:10.4172/2375-4494.1000248

onset. In keeping with the view of adolescence as a time of particular vulnerability to developmental perturbations, cross-sectional studies reveal that regionally specific effects of early stressors in the amygdala are most prominent during adolescence [18]. We therefore examined currently healthy young people who self-reported early exposure to a range of extreme stressors. Self-report measures of early trauma (natural disasters, family illness/death, experiences of bullying etc.) have been previously linked to reduced amygdala volumes in young people [18,26,27], however the impact of such stressors on functional connectivity in youth have not been widely explored [28]. Concurrent examinations of trauma-related changes in both brain structure and functional connectivity have been limited to adult populations or to task-specific activation paradigms [16,29].

The current study employed structural and functional magnetic resonance imaging to examine grey and white matter volume estimates by means of voxel based morphometry (VBM), as well as effective functional connectivity by means of spectral dynamic causal modelling (spectral DCM; spDCM) within the amygdala-hippocampal network in currently-healthy adolescents. Importantly, any neural differences between stress exposed individuals versus unexposed individuals should not be driven by current psychopathology, as all participants were free from current psychopathology.

Materials and Methods

Participants and centers

A large cohort of 298 healthy adolescents [152 males, range: 14-24 years, mean = 19.1 ± 2.9 (SD); 146 females, range: 14-24 years, mean = 19.1 ± 2.9] were scanned over 1½ years at 3 sites: (1) Wellcome Trust Centre for Neuroimaging (WTCN), London, (2) Medical Research Council Cognition and Brain Sciences Unit (MRC CBSU), Cambridge, and (3) Wolfson Brain Imaging Centre (WBIC), Cambridge. The study received ethical approval from the NRES Committee East of England - Cambridge Central (12/EE/0250) and all participants gave written informed consent. This study was conducted by the NeuroScience in Psychiatry Network (NSPN), which addresses how psychiatric disorders are related to abnormal maturation of brain systems.

Selection of participants with histories of abuse and neglect

The Structured Clinical Interview for DSM-IV (SCID) was administered by a trained research assistant and audio recordings were made with the informed consent of participants. During the course of these interviews 29 participants were identified (10 female, mean age 20.45 years) who self-reported histories of trauma (a solitary trauma), including experiences of physical or sexual abuse, having been in a life-threatening situation (e.g. natural disaster, car accident, drowning), physical/sexual assault, death of a parent or sibling or witnessing/hearing about actual or threatened death to others over the course of childhood. The control group (mean age: 20.53 years) was created by matching each trauma-exposed participant to a non-exposed participant in terms of gender, age and parental education levels (as a proxy for socio-economic status). There was no significant difference in handedness between the two groups. Table 1 shows demographic data of participants.

	Trauma-exposed participants (*N* = 29)	Non-exposed participants (*N* = 29)	*p-values*
Age [years]	20.53 ± 2.77 range 16-25	20.45 ± 2.61 range 16-25	0.9087
Sex [Male/Female]	19/10	19/10	1.0000
Parental education [years]	18.05 ± 8.03	16.15 ± 6.18	0.3153

Table 1: Demographic data of selected participants.

Data acquisition and preprocessing

Structural MRI

All multi-parameter maps (MPM) were acquired on 3T whole body MRI systems (Magnetom TIM Trio, Siemens Healthcare, Erlangen, Germany; VB17 software version) operated with the standard 32-channel radio-frequency (RF) receive head coil and RF body coil for transmission. The MPM comprised three multi-echo 3D fast low angle shot (FLASH) scans with PD (TR/α = 23.7 ms/60), T1 (TR/α = 18.7 ms/20^0), and MT (TR/α = 23.7 ms/6^0) - weighted contrast, one RF transmit (B1) field map and one static magnetic (B0) field map scan [30].

The MPM acquisition and pre-processing were developed and optimized in previous studies and are widely described elsewhere [30-36]. The post-processed MT maps resulting from this step were used in our VBM analyses.

Functional MRI

At all three sites, fMRI data were acquired on 3T whole body MRI systems (Magnetom TIM Trio, Siemens Healthcare, Erlangen, Germany; VB17 software version) operated with the standard 32-channel radio-frequency (RF) receive head coil and RF body coil for transmission. 269 contiguous multi-slice images were obtained with a multi-echo-planar sequence (orientation = AC-PC line, number of slices = 34; slice thickness = 3.8 mm; FOV = 240 mm; TE1 = 13 ms; TE2 = 31 ms; TE3 = 48 ms; TR = 2.420 s; flip angle = 90°; matrix size = 64×64×34; voxel size = 3.8×3.8×3.8 mm^3).

The fMRI data were analysed using procedures implemented in Statistical Parametric Mapping (SPM8, Welcome Trust Centre for Neuroimaging, London, UK; http://www.fil.ion.ucl.ac.uk/spm). First, the fMRI data were summed up over the three echoes. Data were then realigned, co-registered, anatomical images were normalized to MNI space, and the resultant normalization matrix was then used to normalize the fMRI data. Finally, the data were visually inspected and spatially smoothed using a 6 mm Gaussian kernel. Ultra-low frequency fluctuations were removed using a high-pass filter (1/128 s, 0.0078 Hz). Confound time-series were extracted from predefined coordinates of extra-cerebral compartments (the pons: x, y, z = 0, -24, -33; and lateral ventricle: x, y, z = 1, -43, 6).

We extracted data exhibiting physiologically-relevant resting-state (i.e. low frequency) dynamics from our region(s) of interest (ROIs): left and right amygdala, and left and right hippocampus, which were anatomically defined using the PickAtlas software (WFU PickAtlas, ANSIR Laboratory, Winston-Salem, NC, USA; http://fmri.wfubmc.edu/software/PickAtlas). The resting-state was thus modelled using a General Linear Model (GLM) with a discrete cosine basis set (GLM-DCT) consisting of 130 functions with frequencies characteristic of resting-state dynamics (0.0078 – 0.1 Hz [37-40]), six nuisance regressors capturing head motion, and the confound time-series from the extra-cerebral compartments. The regional BOLD signal was summarized with the principal eigenvariate (adjusted for confounds: head movements and extra-cerebral compartments) of voxels within 6 mm of the subject's peak coordinate, as identified using statistical parametric mapping. For those familiar with the process of extracting ROIs, this was achieved by using an F-contrast including the discrete

cosine set modelling the resting-state. This procedure allowed us to extract physiologically relevant resting-state data from the anatomically defined regions for each hemisphere.

Spectral dynamic causal modelling (spDCM). Effective connectivity estimates. Spectral dynamic causal modelling (spectral DCM; spDCM) is based on deterministic models that generate predicted crossed spectra from a biophysically plausible model of coupled neuronal fluctuations in a distributed neuronal network [41]. In this setting, the nature of the endogenous fluctuations (and observation noise) has to be parameterized. The most parsimonious and general form, is a power law or scale free form that can be motivated from a large body of work on noise in fMRI [42] and underlying neuronal activity [43,44].

In this study, we intended, first, to improve the description of the endogenous fluctuations (and observation noise) by using auto-regressive (AR) models of different order, and second, to run formal model comparisons in order to select the best AR model, or the best combination of AR models that provide the best balance between accuracy and complexity for explaining the measured data. Accordingly, we modelled endogenous fluctuations (and observation noise) within the amygdala-hippocampal network with AR models from order-1 up to order-16 (N = 1, 2, …, 16). This was done by modifying the deterministic functions that model the neuronal fluctuations (and observation noise) in the source code (they are specified in spm_csd_fmri_mtf.m). Thus, we fitted a total of 16 models to each subject's data. Figure 1 shows the connection scheme employed over this study.

For the analyses presented in this paper, we used spectral DCM for fMRI as implemented in the software package SPM12 (beta version), code release 5831.

Bayesian model selection (BMS)

To select the optimal fluctuation model (given a set of 16 alternatives), we used Bayesian model selection (BMS) for fMRI responses as implemented elsewhere [45,46].

Voxel-based morphometry (VBM)

Grey and white matter volume estimates. For voxel-based morphometry (VBM) analyses, the magnetization transfer (MT) saturation maps were processed in VBM8 (http://dbm.neuro.uni-jena.de/vbm/) with the default settings and classified into different tissue classes: grey matter (GM), white matter (WM), and cerebral-spinal fluid (CSF). The reason for using MT maps is that even though T1w images are commonly used for brain segmentation, the MT maps have been shown to improve the segmentation of subcortical areas [33,47]. Moreover, aiming at optimal anatomical precision we applied the diffeomorphic registration algorithm DARTEL [48]. The warped GM and WM probability maps were scaled by the Jacobian determinants of the deformation fields to account for local compression and expansion [49], resulting in GM and WM volume (GMV/WMV) maps. The GMV/WMV maps were then smoothed by convolution with an isotropic Gaussian kernel of 6 mm full-width-at-half-maximum (FWHM).

We then extracted data from our ROIs which were previously defined using the PickAtlas software (see above). More specifically, we computed the averaged GMV/WMV across voxels within our a priori defined ROIs for each individual. This was followed by a multiple regression analysis.

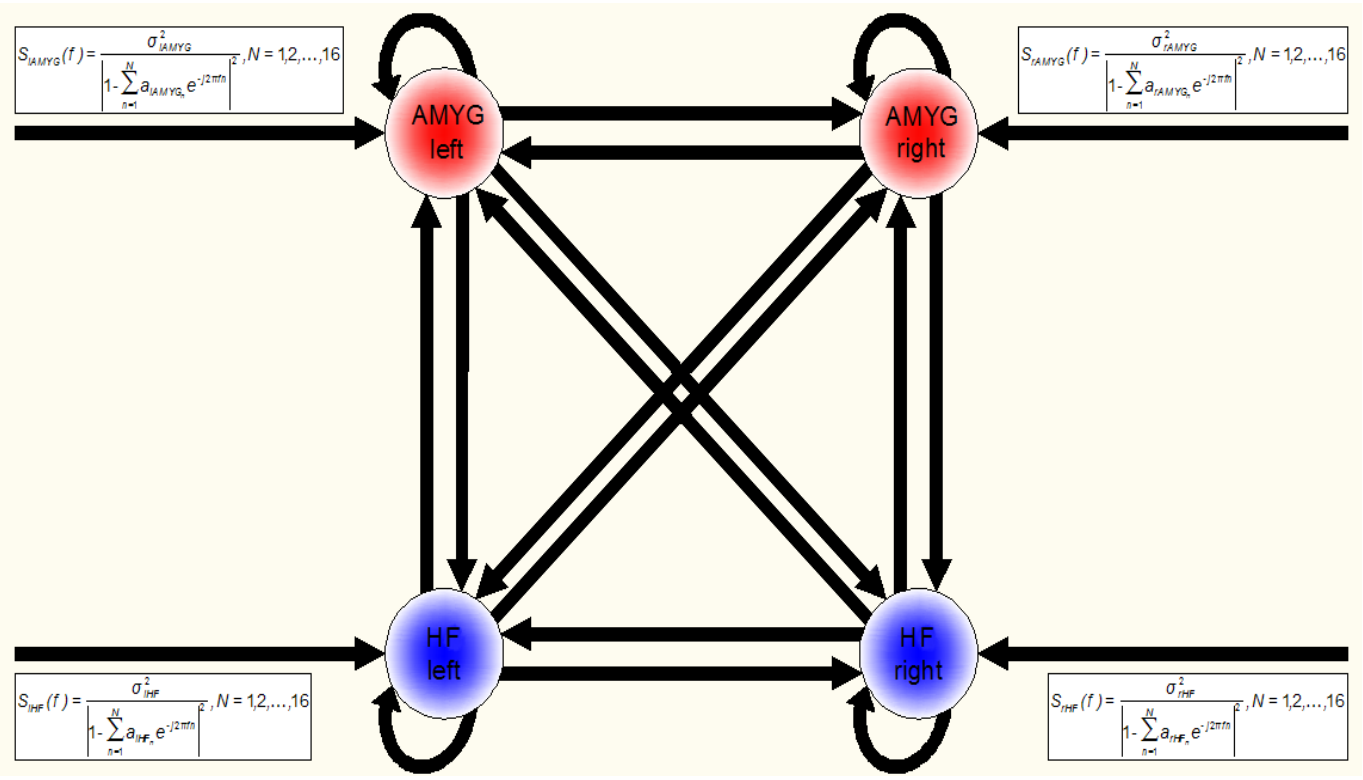

Figure 1: Connection scheme employed over the study. Regions are driven by autoregressive processes of *i*-th order and each order constitutes a model within the set of 16 possible models. AMYG and HF denote amygdala and hippocampal formation respectively.

Multiple linear regression models

To test the hypotheses that spDCM parameter estimates were different between groups, we carried out linear regression analyses.

We first calculated the averaged spDCM parameters from resting-state fMRI data. This was followed by a multiple regression analysis explaining spDCM estimates by a constant, age, differentiating between males and females (in order to identify gender-specific effects), poverty scores, group, and scanner site. The correlation was modelled as:

$$spDCM_i = \beta_1 \times [constant_{male}] + \beta_2 \times [age_{male}] + \beta_3 \times [constant_{female}] + \beta_4 \times [age_{female}] + \beta_5 \times [\text{parental education}] + \beta_6 \times [group] + \beta_7 \times [site] \quad (1)$$

where i runs from 1 to N_p, being $N_p = 84$ the number of spDCM parameter estimates (16 connectivity estimates plus 68 fluctuation estimates).

All independent variables in Eq. (1) were mean corrected. This multiple linear regression was performed on a parameter-by-parameter basis beyond the statistical threshold $p\text{-}value_{FDR} < 0.05$ in the paired t-test of group.

We then considered the same correlation model for grey matter volume (GMV) and white matter volume (WMV) estimates within each ROI separately; we also included the total intracranial volume (TICV) as independent variable.

$$GMV_i = \beta_1 \times [constant_{male}] + \beta_2 \times [age_{male}] + \beta_3 \times [constant_{female}] + \beta_4 \times [age_{female}] + \beta_5 \times [\text{parental education}] + \beta_6 \times [group] + \beta_7 \times [site] + \beta_8 \times [TICV] \text{ parental education} \quad (2)$$

and

$$WMV_i = \beta_1 \times [constant_{male}] + \beta_2 \times [age_{male}] + \beta_3 \times [constant_{female}] + \beta_4 \times [age_{female}] + \beta_5 \times [\text{parental education}] + \beta_6 \times [group] + \beta_7 \times [site] + \beta_8 \times [TICV] \quad (3)$$

where i runs from 1 to N_r, being $N_r = 4$ the number of ROIs.

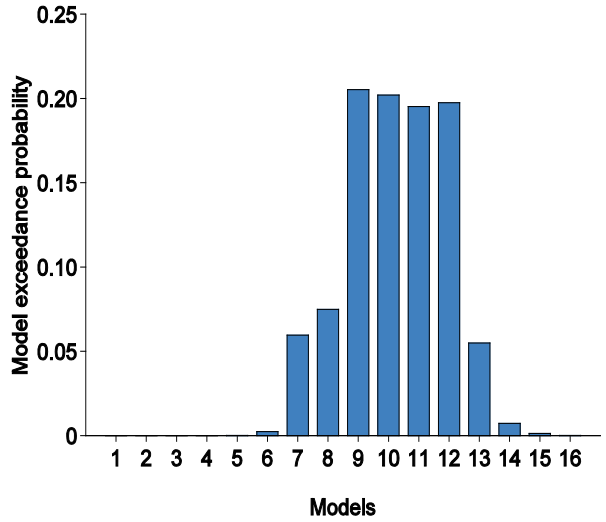

Figure 2: Results of Bayesian model selection on a set of 16 alternative models describing amygdala-hippocampal interactions by means of autoregressive processes of different order in 58 healthy participants (29 trauma-exposed subjects plus 29 pair-wise matched controls).

Results

BMS analyses

We used random effects Bayesian model selection (BMS) to determine, from our model space of 16 alternative spectral DCMs (Figure 1), the model that provided the best balance between accuracy and complexity for explaining the measured data. The analyses did not reveal any winning model in this group of 58 healthy adolescents (29 trauma-exposed participants plus 29 controls), but a subgroup of models having comparable exceedance probabilities.

Figure 2 shows the results of BMS Random Effects (RFX). The exceedance probability of models 9, 10, 11, and 12 (i.e., the probability that this model is a more likely model than any other model considered) was around 0.2. These models describe the neuronal and observation fluctuations by using autoregressive models of order 9, 10, 11, and 12, respectively.

Given the fact that we did not obtain a winning model, we used Bayesian model averaging (BMA) to compute reliable parameter estimates that account for model uncertainty. Recall BMA averages parameter estimates over models by weighting estimates by their corresponding posterior model probabilities [50] (Figure 2).

Statistical Analyses

Following BMA, we used the resulting posterior means from the averaged spectral DCMs for examining correlations (or statistical differences) between spDCM parameter estimates and healthy adolescents with or without a trauma experience. Recall we defined group as a regressor or independent variable in the correlation model accounting for the effects of having or not a trauma experience during childhood (Yes = 1; Not = 0). Table 1 shows the significance levels (*p-values*) for negative associations between group and the averaged spectral DCM estimates (Table 2).

We observed a statistically significant difference in the self-connection within the right amygdala in individuals with a trauma experience compared to controls (*p-value* = 0.0005). Individuals with a trauma experience showed a greater intrinsic connectivity within the right amygdala compared to controls. This connectivity estimate survived multiple comparison problem by means of FDR ($p\text{-}value_{FDR}$ = 0.0425). Recall we correct for 84 parameters or tests.

Following statistical analyses on the sp DCM parameter estimates, we performed statistical analyses on grey and white matter volume estimates within each ROI separately. Tables 2 and 3 show the significance levels (*p-values*) for negative associations between group and GMV, and group and WMV respectively (Tables 3 and 4).

We observed a statistically significant difference in white matter volume (WMV) within the right amygdala in individuals with a trauma experience compared to controls (*p-value* = 0.0208). Individuals with a trauma experience showed a lesser WMV within the right amygdala compared to controls. Even though this difference did not survive survive correction for multiple comparison testing by means of FDR ($p\text{-}value_{FDR}$ = 0.0832), it was very close to significance level (here we corrected for 4 parameters or tests) and more interestingly, it was highlighted the same brain aspect as in previous connectivity analyses: the right amygdala.

At this stage, we may conclude that changes in the self-connection within the right amygdala may be driven by changes in white matter volume within the same aspect. We interpret these findings as suggestive

	$spDCM_i$ = f(group) Negative associations *p-values* (unc.)		$spDCM_i$ = f(group) Negative associations *p-values* (unc.)
(a) Connectivity estimates *16 parameters*		**(b) Fluctuation estimates** *68 parameters*	
		σ^2 (rAMYG)	0.5792
		AR1 (rAMYG)	0.5221
		AR2 (rAMYG)	0.6100
		AR3 (rAMYG)	0.8241
		AR4 (rAMYG)	0.5031
		AR5 (rAMYG)	0.1286
rAMYG → rAMYG	**0.9995***	AR6 (rAMYG)	0.2435
rAMYG → rHF	0.6184	AR7 (rAMYG)	0.1548
rAMYG → lAMYG	0.5160	AR8 (rAYG)	0.1016
rAMYG → lHF	0.0987	AR9 (rAMYG)	0.0824
		AR10 (rAMYG)	0.1284
		AR11 (rAMYG)	0.4827
		AR12 (rAMYG)	0.6835
		AR13 (rAMYG)	0.6617
		AR14 (rAMYG)	0.4974
		AR15 (rAMYG)	0.3944
		AR16 (rAMYG)	0.4785
		σ^2 (rHF)	0.5524
		AR1 (rHF)	0.7178
		AR2 (rHF)	0.6744
		AR3 (rHF)	0.1346
		AR4 (rHF)	0.7284
		AR5 (rHF)	0.8533
rHF → rAMYG	0.6081	AR6 (rHF)	0.8444
rHF → rHF	0.8635	AR7 (rHF)	0.8630
rHF → lAMYG	0.8251	AR8 (rHF)	0.8746
rHF → lHF	0.6159	AR9 (rHF)	0.8661
		AR10 (rHF)	0.7537
		AR11 (rHF)	0.5922
		AR12 (rHF)	0.5791
		AR13 (rHF)	0.5946
		AR14 (rHF)	0.5548
		AR15 (rHF)	0.3854
		AR16 (rHF)	0.3913
		σ^2 (lAMYG)	0.0960
		AR1 (lAMYG)	0.2804
		AR2 (lAMYG)	**0.9937**
		AR3 (lAMYG)	0.3986
		AR4 (lAMYG)	**0.0032**
		AR5 (lAMYG)	0.1085
		AR6 (lAMYG)	0.1608
lAMYG → rAMYG	0.0889	AR7 (lAMYG)	0.5967
lAMYG → rHF	0.2121	AR8 (lAMYG)	**0.9664**
lAMYG → lAMYG	0.7340	AR9 (lAMYG)	0.9443
lAMYG → lHF	0.3730	AR10 (lAMYG)	0.8370
		AR11 (lAMYG)	0.8854
		AR12 (lAMYG)	0.9314
		AR13 (lAMYG)	0.8646
		AR14 (lAMYG)	0.7079
		AR15 (lAMYG)	0.6082
		AR16 (lAMYG)	0.5354
		σ^2 (lHF)	0.7710
		AR1 (lHF)	0.6390
		AR2 (lHF)	0.2017
		AR3 (lHF)	0.3033
		AR4 (lHF)	0.3702
		AR5 (lHF)	0.3286
		AR6 (lHF)	0.4637
lHF → rAMYG	0.4870	AR7 (lHF)	0.4968
lHF → rHF	0.2175	AR8 (lHF)	0.5594
lHF → lAMYG	0.5214	AR9 (lHF)	0.5762
lHF → lHF	0.7818	AR10 (lHF)	0.5695
		AR11 (lHF)	0.6585
		AR12 (lHF)	0.7840
		AR13 (lHF)	0.7306
		AR14 (lHF)	0.6021
		AR15 (lHF)	0.4261
		AR16 (lHF)	0.4617

Table 2: Significance levels (*p-values*) for negative associations between group and spectral DCM parameters: connectivity plus fluctuation estimates. rAMYG, rHF, lAMYG, lHF denote right amygdala, right hippocampal formation, left amygdala, and left hippocampal formation respectively. σ^2 is the variance of the autoregressive process and AR*i* is the *i*-th autoregressive coefficient. Significant p-values (unc.) are highlighted in bold: negative correlations are shown in red, positive correlations in blue, *denotes statistically significant after correction for multiple comparison problem (a total of 84 tests were computed).

	GMV_i = f(group) Negative associations *p-values* (unc.)
GMV (rAMYG)	0.3627
GMV (rHF)	0.2938
GMV (lAMYG)	0.4837
GMV (lHF)	0.1808

Table 3: Significance levels (*p-values*) for negative associations between group and grey matter volume (GMV). rAMYG, rHF, lAMYG, lHF denote right amygdala, right hippocampal formation, left amygdala, and left hippocampal formation respectively.

	WMV_i = f(group) Negative associations *p-values* (unc.)
WMV (rAMYG)	**0.0208**
WMV (rHF)	0.0711
WMV (lAMYG)	0.1790
WMV (lHF)	0.2451

Table 4: Significance levels (*p-values*) for negative associations between group and white matter volume (WMV). rAMYG, rHF, lAMYG, lHF denote right amygdala, right hippocampal formation, left amygdala, and left hippocampal formation respectively. Significant *p-values* (unc.) are highlighted in bold: negative correlations are shown in red, positive correlations in blue.

of abnormal brain maturation after exposure to traumatic experiences.

Discussion

While traumatic early life events might lead to the onset of PTSD or depression, the underlying neurobiological mechanisms have not been yet elucidated. We used voxel based morphometry (VBM) to examine differences in grey and white matter volume, and spectral dynamic causal modelling (spectral DCM; spDCM) to investigate effective connectivity within the amygdala-hippocampal network in healthy adolescents. The primary objective was to identity abnormal patterns of structural-functional brain maturation in young people exposed to traumatic early life experiences in comparison to controls.

Using estimates of grey and white matter volume and effective connectivity, the results indicate greater intrinsic connectivity (i.e. greater excitation) within the right amygdala in individuals with early traumatic experiences compared to controls. Reduced white matter volume (e.g. lesser anatomical wiring) was also observed in the right amygdala for the trauma-exposed group. These findings suggest altered maturation of the right amygdala in young people following trauma exposure.

Based on previous research, our study investigated the impact of trauma on the amygdala-hippocampal network. We did not observe any compelling statistical evidence concerning involvement of the hippocampus, suggesting that amygdala (more specifically the right hemisphere) might be preferentially implicated in traumatic events. It is important to reiterate that the differences we observed should not be attributed to differences in current levels of psychopathology. Instead, the observed maturational brain changes induced by traumatic events might make individuals more susceptible to develop a psychopathology such as PTSD or depression later in life.

A major strength of the present study includes the combined use of various MRI analyses (VBM of grey and white matter, and effective connectivity by means of spectral DCM). Further, inclusion of participants without current psychopathology removes a confound that is present in many previous examinations of this topic. Despite these strengths, some limitations of the study require acknowledgment. First,

the spectral DCM algorithm together with the Bayesian comparison procedure implemented here may be further improved by searching for optimal region-specific fluctuation models (and observation noise) rather than assuming the same generative model across regions (from AR1 up to AR16 processes). Although that approach may have advantages and potentially reveal some other statistical effects, it is computationally very expensive due to estimation of a very large number of models. Second, analyses suggest the use of other statistical correction strategies rather than FDR (e.g. a random field theory approach). The reason for this is that FDR does not take into account autoregressive models (i.e. the temporal structure), nor brain regions (i.e. the spatial structure) and deals with all parameter estimates as independent of each other. Third, VBM is commonly directed at examining gray matter but it can also be used to examine white matter. In the latter case, however, the sensitivity is limited because white matter areas are characterized by large homogeneous regions with only subtle changes in intensity [51]. Finally, the use of the SCID interview to select participants with traumatic life events may be criticized as being too structured (and diagnostically focused), potentially not enabling all former traumatic experiences to be revealed.

In summary, our findings demonstrated abnormal structural-functional maturation of the right amygdala in currently-healthy young people exposed to traumatic events. Together, these findings are suggestive of potential biological markers over the course of adolescence that may have prognostic utility for PTSD or depression. Indeed, our observations, both in white-matter and intrinsic connectivity within right amygdala are very interesting and intriguing, however the reason, i.e. the underlying biological mechanisms that lead to these observations, remain an open question since only a small body of research has been conducted on this topic so far.

Acknowledgements

This work was funded by grants from the Wellcome Trust. Authors acknowledge support by NSPN (NeuroScience in Psychiatry Network) Principals, NSPN Research Assistant team, NSPN Data Management team, and U-CHANGE (Understanding and Characterizing Adolescent-to-Adult Neurodevelopmental Growth Effects) team. D. Bernal-Casas wishes to thanks relatives and friends for their continued moral and financial support.

References

1. Beitchman JH, Zucker KJ, Hood JE, daCosta GA, Akman D, et al. (1992) A review of the long-term effects of child sexual abuse. Child Abuse Negl 16: 101-118.
2. Lupien SJ, McEwen BS, Gunnar MR, Heim C (2009) Effects of stress throughout the lifespan on the brain, behaviour and cognition. Nat Rev Neurosci 10: 434-445.
3. McCrory E, De Brito SA, Viding E (2012) The link between child abuse and psychopathology: a review of neurobiological and genetic research. J R Soc Med 105: 151-156.
4. McEwan K, Waddell C, Barker J (2007) Bringing children's mental health "out of the shadows". CMAJ 176: 471-472.
5. Bremner JD, Randall P, Vermetten E, Staib L, Bronen RA, et al. (1997) Magnetic resonance imaging-based measurement of hippocampal volume in posttraumatic stress disorder related to childhood physical and sexual abuse--a preliminary report. Biol Psychiatry 41: 23-32.
6. van der Werff SJ, Pannekoek JN, Veer IM, van Tol MJ, Aleman A, et al. (2013) Resting-state functional connectivity in adults with childhood emotional maltreatment. Psycho med 43: 1825-1836.
7. Carrion VG, Weems CF, Eliez S, Patwardhan A, Brown W, et al. (2001) Attenuation of frontal asymmetry in pediatric posttraumatic stress disorder. Biol Psychiatry 50: 943-951.
8. Carrion VG, Weems CF, Reiss AL (2007) Stress predicts brain changes in children: a pilot longitudinal study on youth stress, posttraumatic stress disorder, and the hippocampus. Pediatrics 119: 509-516.
9. De Bellis MD, Keshavan MS, Clark DB, Casey BJ, Giedd JN, et al. (1999) A.E. Bennett Research Award. Developmental traumatology. Part II: Brain development. Biological psychiatry 45: 1271-1284.
10. De Bellis MD, Hall J, Boring AM, Frustaci K, Moritz G (2001) A pilot longitudinal study of hippocampal volumes in pediatric maltreatment-related posttraumatic stress disorder. Biol psychiatry 50: 305-309.
11. De Bellis MD, Keshavan MS, Shifflett H, Iyengar S, Beers SR, et al. (2002) Brain structures in pediatric maltreatment-related posttraumatic stress disorder: a sociodemographically matched study. Biol psychiatry 52: 1066-1078.
12. Sripada RK, King AP, Garfinkel SN, Wang X, Sripada CS, et al. (2012) Altered resting-state amygdala functional connectivity in men with posttraumatic stress disorder. J Psychiatry Neurosci 37: 241-249.
13. Bluhm RL, Williamson PC, Osuch EA, Frewen PA, Stevens TK, et al. (2009) Alterations in default network connectivity in posttraumatic stress disorder related to early-life trauma. J Psychiatry Neurosci 34: 187-194.
14. Vythilingam M, Heim C, Newport J, Miller AH, Anderson E, et al. (2002) Childhood trauma associated with smaller hippocampal volume in women with major depression. Am J Psychiatry 159: 2072-2080.
15. Andersen SL, Tomada A, Vincow ES, Valente E, Polcari A, et al. (2008) Preliminary evidence for sensitive periods in the effect of childhood sexual abuse on regional brain development. J Neuropsychiatry Clin Neurosci 20: 292-301.
16. Dannlowski U, Stuhrmann A, Beutelmann V, Zwanzger P, Lenzen T, et al. (2012) Limbic scars: long-term consequences of childhood maltreatment revealed by functional and structural magnetic resonance imaging. Biol Psychiatry 71: 286-293.
17. Gianaros PJ, Jennings JR, Sheu LK, Greer PJ, Kuller LH, et al. (2007) Prospective reports of chronic life stress predict decreased grey matter volume in the hippocampus. Neuroimage 35: 795-803.
18. Korgaonkar MS, Antees C, Williams LM, Gatt JM, Bryant RA, et al. (2013) Early exposure to traumatic stressors impairs emotional brain circuitry. PLoS One 8: e75524.
19. Cohen RA, Grieve S, Hoth KF, Paul RH, Sweet L, et al. (2006) Early life stress and morphometry of the adult anterior cingulate cortex and caudate nuclei. Biol Psychiatry 59: 975-982.
20. Baker LM, Williams LM, Korgaonkar MS, Cohen RA, Heaps JM, et al. (2013) Impact of early vs. late childhood early life stress on brain morphometrics. Brain Imaging Behav 7: 196-203.
21. Nooner KB, Mennes M, Brown S, Castellanos FX, Leventhal B, et al. (2013) Relationship of trauma symptoms to amygdala-based functional brain changes in adolescents. J Trauma Stress 26: 784-787.
22. Vaisvaser S, Lin T, Admon R, Podlipsky I, Greenman Y, et al. (2013) Neural traces of stress: cortisol related sustained enhancement of amygdala-hippocampal functional connectivity. Front Hum Neurosci 7: 313.
23. Casey BJ, Giedd JN, Thomas KM (2000) Structural and functional brain development and its relation to cognitive development. Biol Psychol 54: 241-257.
24. Knudsen EI (2004) Sensitive periods in the development of the brain and behavior. J Cogn Neurosci 16: 1412-1425.
25. Blakemore SJ (2012) Imaging brain development: the adolescent brain. Neuroimage 61: 397-406.
26. Aas M, Navari S, Gibbs A, Mondelli V, Fisher HL, et al. (2012) Is there a link between childhood trauma, cognition, and amygdala and hippocampus volume in first-episode psychosis? Schizophr Res 137: 73-79.
27. De Brito SA, Viding E, Sebastian CL, Kelly PA, Mechelli A, et al. (2013) Reduced orbitofrontal and temporal grey matter in a community sample of maltreated children. J Child Psychol Psychiatry 54: 105-112.
28. Dean AC, Kohno M, Hellemann G, London ED (2014) Childhood maltreatment and amygdala connectivity in methamphetamine dependence: a pilot study. Brain Behav 4: 867-876.
29. Ganzel BL, Kim P, Glover GH, Temple E (2008) Resilience after 9/11: multimodal neuroimaging evidence for stress-related change in the healthy adult brain. Neuroimage 40: 788-795.
30. Weiskopf N, Lutti A, Helms G, Novak M, Ashburner J, et al. (2011) Unified segmentation based correction of R1 brain maps for RF transmit field inhomogeneities (UNICORT). Neuroimage 54: 2116-2124.

31. Helms G, Dathe H, Dechent P (2008) Quantitative FLASH MRI at 3T using a rational approximation of the Ernst equation. Magn Reson Med 59: 667-672.

32. Helms G, Dathe H, Kallenberg K, Dechent P (2008) High-resolution maps of magnetization transfer with inherent correction for RF inhomogeneity and T1 relaxation obtained from 3D FLASH MRI. Magn Reson Med 60: 1396-1407.

33. Helms G, Draganski B, Frackowiak R, Ashburner J, Weiskopf N (2009) Improved segmentation of deep brain grey matter structures using magnetization transfer (MT) parameter maps. Neuroimage 47: 194-198.

34. Helms G, Dathe H, Weiskopf N, Dechent P (2011) Identification of signal bias in the variable flip angle method by linear display of the algebraic Ernst equation. Magn Reson Med 66: 669-677.

35. Lutti A, Hutton C, Finsterbusch J, Helms G, Weiskopf N (2010) Optimization and validation of methods for mapping of the radiofrequency transmit field at 3T. Magn Reson Med 64: 229-238.

36. Lutti A, Stadler J, Josephs O, Windischberger C, Speck O, et al. (2012) Robust and fast whole brain mapping of the RF transmit field B at 7T. PLoS One 7: e32379.

37. Biswal B, Yetkin FZ, Haughton VM, Hyde JS (1995) Functional connectivity in the motor cortex of resting human brain using echo-planar MRI. Magn Reson Med 34: 537-541.

38. Fransson P (2005) Spontaneous low-frequency BOLD signal fluctuations: an fMRI investigation of the resting-state default mode of brain function hypothesis. Hum brain mapp 26: 15-29.

39. Fox MD, Raichle ME (2007) Spontaneous fluctuations in brain activity observed with functional magnetic resonance imaging. Nat Rev Neurosci 8: 700-711.

40. Deco G, Jirsa VK, McIntosh AR (2011) Emerging concepts for the dynamical organization of resting-state activity in the brain. Nat Rev Neurosci 12: 43-56.

41. Friston KJ, Kahan J, Biswal B, Razi A (2014) A DCM for resting state fMRI. Neuroimage 94: 396-407.

42. Bullmore E, Long C, Suckling J, Fadili J, Calvert G, et al. (2001) Colored noise and computational inference in neurophysiological (fMRI) time series analysis: resampling methods in time and wavelet domains. Hum brain mapp 12: 61-78.

43. Shin CW, Kim S (2006) Self-organized criticality and scale-free properties in emergent functional neural networks. Physical review E, Statistical, nonlinear, and soft matter physics 74: 045101.

44. Stam CJ, de Bruin EA (2004) Scale-free dynamics of global functional connectivity in the human brain. Hum Brain Mapp 22: 97-109.

45. Penny WD, Stephan KE, Mechelli A, Friston KJ (2004) Comparing dynamic causal models. Neuroimage 22: 1157-1172.

46. Stephan KE, Penny WD, Daunizeau J, Moran RJ, Friston KJ (2009) Bayesian model selection for group studies. Neuroimage 46: 1004-1017.

47. Tardif CL, Collins DL, Pike GB (2009) Sensitivity of voxel-based morphometry analysis to choice of imaging protocol at 3 T. Neuroimage 44: 827-838.

48. Ashburner J (2007) A fast diffeomorphic image registration algorithm. Neuroimage 38: 95-113.

49. Ashburner J, Friston KJ (2000) Voxel-based morphometry--the methods. Neuroimage 11: 805-821.

50. Penny WD, Stephan KE, Daunizeau J, Rosa MJ, Friston KJ, et al. (2010) Comparing families of dynamic causal models. PLoS Comput Biol 6: e1000709.

51. Kurth F, Luders E, Gaser C (2015) Voxel-Based Morphometry. In: Toga AW (Edn). Brain Mapping. Academic Press: Waltham pp: 345-349.